EUROPEAN ORGANIZATION FOR NUCLEAR RESEARCH

An Improved Theoretical Prediction for the 2–Jet Rate in e$^+$e$^-$ Annihilation

Günther Dissertori
Institute of Experimental Physics, Innsbruck, Austria

Michael Schmelling
CERN, Geneva, Switzerland

Abstract

We show that an Ansatz to resum all leading and next–to–leading logarithms in the theoretical prediction for the 2–jet rate in $e^+e^- \rightarrow$ hadrons, where jets are defined with the k_t–algorithm, is consistent with a full $\mathcal{O}(\alpha_s^2)$ calculation done by Monte Carlo integration. From the asymptotic behaviour of the full $\mathcal{O}(\alpha_s^2)$ calculation we extract the subleading coefficient G_{21} and the constant C_2.

1 Introduction

The study of global event shape variables in e^+e^- annihilation is one of the most precise methods to determine the strong coupling constant α_s. Here the very accurate data obtained at LEP have led to a situation, where the error of α_s is dominated by the theoretical uncertainties [1], related to uncalculated higher order terms in the perturbative expansion or to non-perturbative hadronization effects. For α_s–measurements based on the 2–jet rate R_2 the theoretical error comes mainly from the perturbative sector, i.e. any improvement in the perturbative prediction would lead to a better measurement of α_s.

At present, full perturbative calculations for any infrared and collinear safe event shape variable exist only up to $\mathcal{O}(\alpha_s{}^2)$ [2]. For some variables also leading and next–to–leading logarithms have been resummed to all orders in α_s [3, 4, 5, 6]. See [7] for a detailed description of these resummation techniques, which use the coherent branching algorithm to next–to–leading logarithmic accuracy.

If calculated with the k_t–algorithm [8, 9, 6] based on the resolution parameter

$$y_{ij} = \frac{2 \min(E_i^2, E_j^2)}{E_{cm}^2}(1 - \cos \Theta_{ij}), \qquad (1)$$

the perturbative prediction for R_2 is known to exponentiate, which allows to resum leading and next–to–leading logarithms $L = -\ln(y_3)$, where y_3 is the resolution parameter where the event undergoes the transition from a 3–jet to a 2–jet event. Theoretical calculations [6] are available, which resum all leading and part of the next–to–leading logarithms. This work describes an Ansatz for the resummed prediction of R_2, motivated by the exponentiation behaviour of similar terms for other variables [3, 4, 5], which tries to include the missing next–to–leading logarithmic contributions.

2 The Theoretical Framework

In order to simplify the expressions describing the theoretical prediction for R_2, it is convenient to introduce the colour factor ratios f_A and f_T and to redefine the strong coupling constant by absorbing into it a factor of $C_F/2\pi$. This leads to the definitions:

$$f_A = \frac{C_A}{C_F} \quad , \quad f_T = N_f \frac{T_F}{C_F} \quad \text{and} \quad \overline{\alpha}_s = \frac{\alpha_s C_F}{2\pi}. \qquad (2)$$

For the following the number of active quark flavours is N_f=5. The QCD values for the colour factors are C_F=4/3, C_A=3 and T_F=1/2.

According to general theorems [10] the perturbative prediction for the cumulative cross section of any event shape variable y, which vanishes in the limit of perfect 2–jet topologies, can be expressed in the form,

$$R(L) = \frac{\sigma(-\ln(y) > L)}{\sigma_{tot}} = \left(1 + \sum_{i=1}^{\infty} C_i \overline{\alpha}_s^i\right) \exp\left(\sum_{n=1}^{\infty} \sum_{m=1}^{2n} G_{nm} \overline{\alpha}_s^n L^m\right) + \sum_{k=1}^{\infty} \overline{\alpha}_s^k D_k(L), \qquad (3)$$

where for clarity any explicit dependence on the renormalization scale μ^2 is suppressed. The $D_k(L)$ are regular functions which vanish in the limit $L \to \infty$. The terms in the double sum are

classified as leading logarithms (LL) for $m > n$, next–to–leading logarithms (NLL) for $m = n$ and sub–leading for $m < n$. Exponentiation of the perturbative prediction means $G_{nm} = 0$ for $m > n + 1$. In this case one can write

$$\sum_{n=1}^{\infty} \sum_{m=1}^{n+1} G_{nm} \overline{\alpha}_s^n L^m = \ln \Sigma(\overline{\alpha}_s, L) = L g_1(\overline{\alpha}_s L) + g_2(\overline{\alpha}_s L) + \cdots. \tag{4}$$

Thus the function $L g_1(\overline{\alpha}_s L)$ resums all the LL contributions $\overline{\alpha}_s^n L^{n+1}$, $g_2(\overline{\alpha}_s L)$ contains the NLL terms $\overline{\alpha}_s^n L^n$ and the remainder the sub–leading corrections.

The resummed expression for $\ln \Sigma_{R_2(y_3)}$, where $R_2(y_3)$ is the 2–jet rate as function of the cut–off y_3 is given in [6] as

$$\ln \Sigma_{R_2(y_3)} = -2 \int_{s y_3}^{s} \frac{dq^2}{q^2} \overline{\alpha}_s(q^2) \left(\ln \frac{s}{q^2} - \frac{3}{2} \right) . \tag{5}$$

The explicit dependence on the renormalization scale μ^2 can be obtained by expanding $\overline{\alpha}_s(q^2)$ in terms of $\overline{\alpha}_s(\mu^2)$, using the solution of the renormalization group equation given in [11]

$$\overline{\alpha}_s(q^2) = \frac{\overline{\alpha}_s(\mu^2)}{w} \left(1 - \frac{b_1}{b_0} \frac{\overline{\alpha}_s(\mu^2)}{w} \ln w \right) \quad , \quad w = 1 - b_0 \overline{\alpha}_s(\mu^2) \ln \frac{\mu^2}{q^2} \quad , \tag{6}$$

with

$$b_0 = \frac{11}{6} f_A - \frac{2}{3} f_T \quad \text{and} \quad b_1 = \frac{17}{6} f_A^2 - \left(\frac{5}{3} f_A + 1 \right) f_T . \tag{7}$$

One of the main ingredients of the coherent branching algorithm is the Altarelli-Parisi (AP) splitting function $P_{qq}(\overline{\alpha}_s, z)$ [12], which describes the parton branching $q \to qg$ as function of the longitudinal momentum fraction z. In the infrared limit it is given by

$$P_{qq}(\overline{\alpha}_s, z \to 1) = \frac{2}{1 - z} \left(\overline{\alpha}_s + \overline{\alpha}_s^2 K \right) \tag{8}$$

where

$$K = f_A \left(\frac{67}{18} - \frac{\pi^2}{6} \right) - f_T \frac{10}{9} = f_A K_A + f_T K_T . \tag{9}$$

For the calculation in [6] only the first order part of Eq.(8) has been used, which gives rise to the terms $\overline{\alpha}_s(q^2) \ln(s/q^2)$ under the integral Eq.(5). The term $\propto 3/2$ in Eq.(5) comes from the (+)-regularization [13] of the AP splitting function.

Motivated by the fact that for other event shape variables also the next–to–leading part of the AP splitting function exponentiates, we assume that the same holds for the 2–jet rate. The functional form of Eq.(8) suggests the following Ansatz:

$$\ln \Sigma_{R_2(y_3)} = -2 \int_{s y_3}^{s} \frac{dq^2}{q^2} \left\{ \overline{\alpha}_s(q^2) \left(\ln \frac{s}{q^2} - \frac{3}{2} \right) + \overline{\alpha}_s^2(q^2) K \ln \frac{s}{q^2} \right\}. \tag{10}$$

Doing the integration and dropping all subleading terms, the result can be expressed as

$$\ln \Sigma_{R_2(y_3)} = L g_1(x) + g_2(x) + x^2 g_1'(x) \ln \frac{\mu^2}{s} \tag{11}$$

2

with $L = -\ln(y_3)$ and $x = \overline{\alpha}_s(\mu^2)b_0 L$. The prime in $g_1'(x)$ stands for derivative with respect to the given argument. The functions $g_1(x)$ and $g_2(x)$ are:

$$g_1(x) = \frac{2}{b_0}\left(1 + \frac{\ln(1-x)}{x}\right) \tag{12}$$

$$g_2(x) = -\frac{3}{b_0}\ln(1-x) - \frac{2K}{b_0^2}\left(\frac{x}{1-x} + \ln(1-x)\right) + \frac{2b_1}{b_0^3}\left(\frac{x + \ln(1-x)}{1-x} + \frac{1}{2}\ln^2(1-x)\right) \tag{13}$$

Expanding the above functions in powers of $\overline{\alpha}_s$ one sees that the terms proportional to K only contribute to $\mathcal{O}(\overline{\alpha}_s^2)$. The additional terms are proportional to the colour factors C_A and T_F, expressing the fact that we have included missing NLL terms coming from higher order corrections to the fundamental $q \to qg$ branching. The renormalization scale dependence of $\ln\Sigma_{R_2(y_3)}$ is entirely determined by the LL function $g_1(x)$, i.e. it is independent of K. It is worth noting [14] that the additional NLL terms proportional to K could also be generated in the original formula [6] by choosing the renormalization scale $\ln\mu^2/s = K/b_0$.

3   Comparison with the Full $\mathcal{O}(\alpha_s^2)$ Calculation

In the following the renormalization scale will be set to $\mu^2 = s$. The leading coefficients G_{nm} of the full perturbative prediction Eq.(3) can be read off by expanding the result for $\ln\Sigma_{R_2(y_3)}$ in powers of x:

$$\ln\Sigma_{R_2(y_3)} = \frac{x}{b_0}(3-L) + \left(\frac{x}{b_0}\right)^2\left(\frac{3b_0}{2} - K - \frac{2b_0}{3}L\right) + \mathcal{O}(x^3). \tag{14}$$

From this the leading coefficients are read off as $G_{12} = -1$, $G_{11} = 3$, $G_{23} = -2b_0/3$ and $G_{22} = 3b_0/2 - K$. The coefficient C_1 has been obtained in [9] by computing the 3–jet fraction $R_3(L)$ in lowest order[1]. There one finds

$$C_1 = -6\ln 2 - \frac{5}{2} + \frac{\pi^2}{6} \quad . \tag{15}$$

The exact expressions for $D_2(L), G_{21}, C_2$ are not known. The function $D_1(L)$ can be extracted from the integral of the analytical first order result given in the appendix.

For the comparison with the Monte Carlo integration of the second order matrix element it is more convenient to use the differential cross section

$$\frac{1}{\sigma_0}\frac{d\sigma}{dL} = -\frac{\sigma_{had}}{\sigma_0}\frac{dR_2}{dL} \quad . \tag{16}$$

Here σ_0 is the Born cross section for $e^+e^- \to q\overline{q}$, which is related to the full hadronic cross section σ_{had} by

$$\frac{\sigma_{had}}{\sigma_0} = 1 + \frac{3}{2}\overline{\alpha}_s + \mathcal{O}(\overline{\alpha}_s^2) \quad . \tag{17}$$

---

[1] Note that formula (8) in reference [9] can not be correct because the 3–jet fraction does not vanish at the phase space boundary $y_3 = 1/3$. However, it has been checked numerically that the asymptotic behaviour $L \to \infty$ and thus the constant C_1 is reproduced correctly.

By inserting the values for the coefficients G_{nm} and separating the individual colour factor contributions one finally gets:

$$
\begin{aligned}
\frac{1}{\sigma_0}\frac{d\sigma}{dL} \; = \; & \overline{\alpha}_s && [\, 2L - 3 + S_1(L) \,] \\
+ \; & \overline{\alpha}_s^2 && \left[-2L^3 + 9L^2 - (\; 6 \; - 2C_1 \;)L - G_{21,F} + S_F(L) - 3C_1 - \frac{9}{2} + \frac{3}{2}S_1(L) \right] \\
+ \; & \overline{\alpha}_s^2 f_A && \left[\quad \frac{11}{3}L^2 - (\frac{11}{2} - 2K_A)L - G_{21,A} + S_A(L) \right] \\
+ \; & \overline{\alpha}_s^2 f_T && \left[\quad -\frac{4}{3}L^2 + (\; 2 \; + 2K_T)L - G_{21,T} + S_T(L) \right] \; + \; \mathcal{O}(\overline{\alpha}_s^3)
\end{aligned}
\tag{18}
$$

The colour factor decomposition of K is given in Eq.(9). Similarly one has $G_{21} = G_{21,F} + f_A G_{21,A} + f_T G_{21,T}$. The functions $S_*(L)$, $* = F, A, T$, are defined by derivatives of the functions D_1 and D_2 introduced in Eq.(3) as $-D_1'(L) = S_1(L)$ and $-D_2'(L) = S_F(L) + f_A S_A(L) + f_T S_T(L)$.

3.1 The Numerical Calculation

The differential cross section can be written in the form

$$
\frac{1}{\sigma_0}\frac{d\sigma}{dL} = \overline{\alpha}_s a(L) + \overline{\alpha}_s^2 \left[b_F(L) + f_A b_A(L) + f_T b_T(L) \right] \quad .
\tag{19}
$$

We have used a modified version of the Monte Carlo program EVENT [15] to integrate the second order QCD ERT matrix elements [16] in order to calculate the a and b coefficients. The program has been changed with respect to the user interface, the random number generator and to allow to get the coefficients of each colour factor separately. In total we have generated 33.6214×10^9 events and stored the functions a, b in bins of width $\Delta L = 0.2$. The results for the E–scheme are tabulated in Tab. 2 for the L range over which the calculations are stable. The integration was done also for the E0, P and P0–schemes [17]. Tabulated coefficients for these schemes can be obtained from the authors. The first order prediction $a(L)$ is scheme independent. Figure 1 shows how the second order coefficients for the different schemes approach each other at large L. With exception of b_F for the P0–scheme all curves come together at large L, indicating that up to $\mathcal{O}(\overline{\alpha}_s^2)$ also the subleading coefficients $G_{21,A}$ and $G_{21,T}$ are independent of the recombination scheme. The following is based only on the results obtained for the E–scheme.

The functions a, b contain all LL, NLL and subleading terms correctly up to $O(\overline{\alpha}_s^2)$. Thus a comparison of the numerical calculation with the expansion Eq.(18) at high L allows to test the Ansatz Eq.(10). In this region the two calculations should only differ by a constant plus a contribution which vanishes asymptotically.

The function a was compared with the full analytical calculation given in the appendix. The calculations agree with each other over the whole L range (Fig. 2a), giving confidence in the precision of the numerical integration. The functions b_* follow the expected behaviour at large L as can be seen from Figs. 2b, 2c and 2d. At low L the influence of subleading terms is clearly visible. In the case of the coefficients $b_A(L)$ and $b_T(L)$ also the effect of setting $K = 0$ is shown, demonstrating the need of the additional term in the Ansatz Eq.(10) and the sensitivity to this NLL contribution.

4

3.2 Study of the Leading-Order non-Logarithmic Terms

In the limit of large L the result given in the appendix for the differential 2-jet rate can be expanded to yield

$$\frac{1}{\sigma_0}\frac{d\sigma^{1st}}{dL} = \overline{\alpha}_s \left(2L - 3 + Ae^{-L/2} + Be^{-L} + \cdots \right) \tag{20}$$

with

$$A = 4\sqrt{2} + \ln(3 - 2\sqrt{2}) \quad \text{and} \quad B = 18\ln 2 - 1 - 4L \quad . \tag{21}$$

The LL and NLL terms are the same as those in Eq.(18), and one finds the non-logarithmic terms $S_1(L)$ to behave like

$$S_1(L) = \frac{1}{\sigma_0}\frac{d\sigma^{1st}}{dL} - \overline{\alpha}_s\left(2L - 3\right) = \overline{\alpha}_s\left(Ae^{-L/2} + Be^{-L} + \cdots\right). \tag{22}$$

The inset in Fig. 2 shows the relative contribution of $S_1(L)$ with respect to the full first order prediction as function of L. It can be seen that this contribution falls below the 1% level only at $L \approx 8$, which corresponds to $y_3 \approx 3.35 \times 10^{-4}$.

3.3 Determination of the Coefficients G_{21} and C_2

Having subtracted all the known terms as given in Eq.(18) from the numerically obtained coefficients b_*, the resulting differences Δb_* are plotted in Fig. 3. Assuming the asymptotic behaviour of all subleading functions $S_*(L)$ to be the same as for $S_1(L)$, we have fitted functions

$$a_0 + a_1 e^{-L/2} + a_2 e^{-L} \tag{23}$$

separately to each Δb_* in the asymptotic region. This allows to extract the subleading coefficients $G_{21,*}$ for each colour factor. The results are listed in Tab. 1.

$*$	$G_{21,*}$	$\pm$	$stat$	$\pm$	$syst$	Fit Range in L
F	-16.081	$\pm$	0.277	$\pm$	1.304	$5.6 \to 10.0$
A	-4.551	$\pm$	0.081	$\pm$	0.296	$5.6 \to 10.0$
T	0.900	$\pm$	0.018	$\pm$	0.087	$7.4 \to 12.0$

Table 1: Fitted values for the subleading coefficients $G_{21,*}$.

The determination of the coefficients $G_{21,*}$ was done as follows: Fixing the upper limit of the fit range and decreasing the lower limit as long as the χ^2/N_{df} is near to one, we first fit only the parameter a_0. The other two are set to zero. The result for $G_{21,*}$ obtained with the largest fit range is retained. Then the procedure is repeated with a_1 as additional free parameter and finally with all three varying freely. As central value the result $G_{21,*}$ is chosen, which was obtained with the a_0 and a_1 allowed to vary and a_2 set to zero. The statistical error reflects the finite Monte Carlo statistics, the systematic error is the larger of the differences to the other variants. Combining the coefficients for the individual different colour factors yields for QCD

$$G_{21} = -24.633 \pm 1.509 \quad .$$

Using the fitted value of G_{21}, the procedure described above is applied to the difference between the numerically obtained 2–jet rate $R_2(L)$ and the second order expansion of Eq.(3). Taking the correlations between the bins of the R_2–distribution into account we obtain the following result for the QCD coefficient C_2:

$$C_2 = 99.12 \pm 2.75 + 4.30(G_{21} - G_{21}^{var}) \quad .$$

The third term parametrizes the change in C_2 when the central value G_{21} is varied to G_{21}^{var}. Figure 4 illustrates the effect of adding G_{21} and C_2 to the LL plus NLL prediction of the 2–jet rate. The above results are consistent with another recent calculation [18], however, the errors given there are rather large and the possible effect of non-logarithmic contribution was neglected.

4   A Fit for $\alpha_{\mathrm{s}}(\mathbf{M}_{\mathbf{Z}}^2)$

The effect of the improved prediction on a measurement of the strong coupling constant was studied by applying the same procedure used in [11] to the y_3 distribution generated with the JETSET [19] Monte Carlo model. It turns out, that a measurement based on the improved theory lowers the central value of α_s by 60% of the theoretical uncertainty. The relative theoretical error, determined according to the prescription given in [11], remains constant at $\Delta\alpha_s/\alpha_s = 0.038$.

Knowing the subleading term G_{21} and the constant C_2 it is now also possible to apply the "intermediate" matching scheme as described in [11] to the case of the y_3 distribution. The results are very similar to the results obtained for the $\ln R$ scheme. The same observation was made in [11] for the event shape variables Thrust and Heavy Jet Mass.

5   Summary

We have shown that a new Ansatz for the resummed prediction for the 2–jet rate, based on the assumption that the infrared singular part of the next–to–leading AP splitting function P_{qq} exponentiates, is consistent with a full $\mathcal{O}(\alpha_s{}^2)$ calculation obtained from a high statistics Monte Carlo integration of the ERT matrix elements. Using this Ansatz we are able to extract the subleading coefficients by fitting the asymptotic tail of the numerical calculation. The results for the E–scheme are $G_{21} = -24.633 \pm 1.509$ and $C_2 = 99.12 \pm 2.75$, where C_2 is a function of G_{21}. The numerical values apply for a perturbative expansion in $\overline{\alpha}_s = \alpha_s C_F/2\pi$. An α_s-measurement based on the new theoretical prediction and the same procedure as used in [11] lowers the central value of α_s by 60% of the theoretical error. The relative size of the theoretical uncertainty remains constant.

Acknowledgements

Appendix: The Differential 2–Jet Rate in Leading Order

The differential 2–jet rate in first order is obtained by calculating the integral

$$\frac{d\sigma^{1st}}{dy_3} = \int dx_q dx_{\bar{q}} \frac{d^2\sigma}{dx_q dx_{\bar{q}}} \delta(y_3 - \hat{y}_3(x_q, x_{\bar{q}})) \tag{24}$$

over the appropriate phase space, where the matrix element for $e^+e^- \to q\bar{q}g$ is [20]

$$\frac{1}{\sigma_0} \frac{d^2\sigma}{dx_q dx_{\bar{q}}} = \overline{\alpha}_s \frac{x_q^2 + x_{\bar{q}}^2}{(1 - x_q)(1 - x_{\bar{q}})} \quad . \tag{25}$$

Here x_q and $x_{\bar{q}}$ are the scaled energies of the quark and the anti–quark respectively, defined as $x = 2E/E_{CM}$. For energy ordered configurations $x_1 > x_2 > x_3$ the variable $\hat{y}_3$ determined by the k_t-algorithm is given by

$$\hat{y}_3 = (1 - x_1)\frac{x_3}{x_2} \quad . \tag{26}$$

One obtains:

$$\frac{1}{\sigma_0} \frac{d\sigma^{1st}}{dy_3} = \overline{\alpha}_s f_3(y_3) \tag{27}$$

with

$$
\begin{aligned}
f_3(y_3) &= -7 + 12b - \frac{3}{y_3} + 16y_3 - \frac{(1 - y_3)(12y_3 - 12by_3 - 5y_3^2)}{(2 - 2b - y_3)^2} + \frac{6 - 8y_3 + 2y_3^2}{1 - b + y_3} \\
&+ \frac{b^2 + 2by_3 + 4y_3^2}{1 - y_3} - \frac{4\sqrt{y_3}}{1 - y_3} \ln\left(\frac{1 + \sqrt{y_3}}{1 - \sqrt{y_3}}\right) - \frac{1}{\sqrt{y_3}} \frac{1 + y_3}{1 - y_3} \ln\left(\frac{2 - 2b - \sqrt{y_3}}{2 - 2b + \sqrt{y_3}}\right) \\
&+ \frac{2}{\sqrt{y_3}} \ln\left(\frac{\sqrt{y_3} - 1 + b}{\sqrt{y_3} + 1 - b}\right) + 2\frac{1 + y_3}{1 - y_3} \ln\left(\frac{1 - y_3}{2}\right) + \frac{2 + y_3}{y_3} \ln\left(2\frac{1 - y_3}{2 - b}\right) \\
&+ \frac{6 - 10y_3 + 8y_3^2}{1 - y_3} \ln\left(2\frac{2 - 2b - y_3}{1 - y_3}\right) - \frac{4}{y_3(1 - y_3)} \ln\left(\frac{y_3}{1 - b}\right) \\
&- \frac{1 + y_3}{1 - y_3} \ln(2by_3 - y_3) + (8 - 4y_3) \ln\left(\frac{2y_3}{1 - b + y_3}\right)
\end{aligned}
\tag{28}
$$

and $b = 1 + y_3/4 - \sqrt{y_3/2 + y_3^2/16}$.

References

[1] M. Schmelling, Physica Scripta **51** (1995) 683.

[2] Z. Kunszt, P. Nason, G. Marchesini and B.R. Webber, in "Z Physics at LEP1", CERN 89–08, vol. 1 , p. 373.

[3] S. Catani, G. Turnock, B.R. Webber and L. Trentadue, Phys. Lett. **B263** (1991) 491.

[4] S. Catani, G. Turnock and B.R. Webber, Phys. Lett. **B272** (1991) 368.

[5] S. Catani, G. Turnock and B.R. Webber, Phys. Lett. **B295** (1992) 269.

[6] S. Catani, Y.L. Dokshitzer, M. Olsson, G. Turnock and B.R. Webber, Phys. Lett. **B269** (1991) 432.

[7] S. Catani, L. Trentadue, G. Turnock and B.R. Webber, CERN Preprint CERN–TH.6640/92 (1992), Cavendish–HEP–91/11.

[8] Y.L. Dokshitzer, Contribution to the Workshop on Jets at LEP and HERA, Durham (1990).

[9] N. Brown, W.J. Stirling, Z. Phys. **C53** (1992) 629

[10] F. Bloch, A. Nordsieck, Phys. Rev. **52** (1937) 54;
T. Kinoshita, J. Math. Phys. **3** (1962) 650;
T.D. Lee, M. Nauenberg, Phys. Rev. **133** (1964) 1549.

[11] ALEPH Collaboration, D. Decamp *et al.*, Phys. Lett. **B284** (1992) 163.

[12] G. Altarelli, G. Parisi, Nucl. Phys. **B126** (1977) 298.

[13] G. Altarelli, Phys. Rep. **81** (1982) 1.

[14] S. Catani, G. Marchesini, B.R. Webber, Nucl. Phys. **B349** (1991) 635.

[15] P. Nason, private communication.

[16] R.K. Ellis, D.A. Ross, A.E. Terrano, Nucl. Phys. **B178** (1981) 421.

[17] S. Bethke, Z. Kunszt, D.E. Soper, W.J. Stirling, Nucl. Phys. **B370** (1992) 310.

[18] G. Kramer and H. Spiessberger, Preprint DESY 95-097.

[19] T. Sjöstrand, Comp. Phys. Comm. **27** (1982) 243;
T. Sjöstrand, Comp. Phys. Comm. **28** (1983) 229;
T. Sjöstrand and M. Bengtson, Comp. Phys. Comm. **43** (1987) 367.

[20] J. Ellis, M.K. Gaillard and G.G. Ross, Nucl. Phys. **B111** (1976) 253.

L	$a \pm stat$	$b_F \pm stat$	$b_A \pm stat$	$b_T \pm stat$
$1.0 - 1.2$	0.07762 ± 0.00001	-0.1044 ± 0.0005	0.4048 ± 0.0003	-0.26399 ± 0.00004
$1.2 - 1.4$	0.54700 ± 0.00002	1.6420 ± 0.0011	3.4988 ± 0.0006	-1.70748 ± 0.00010
$1.4 - 1.6$	0.98268 ± 0.00003	2.9449 ± 0.0016	6.4687 ± 0.0008	-3.09932 ± 0.00015
$1.6 - 1.8$	1.36284 ± 0.00004	3.7449 ± 0.0021	9.3027 ± 0.0011	-4.37929 ± 0.00020
$1.8 - 2.0$	1.71658 ± 0.00004	4.1990 ± 0.0027	12.2312 ± 0.0014	-5.63718 ± 0.00025
$2.0 - 2.2$	2.05878 ± 0.00005	4.2715 ± 0.0034	15.3390 ± 0.0017	-6.92511 ± 0.00031
$2.2 - 2.4$	2.39721 ± 0.00006	3.8738 ± 0.0041	18.6777 ± 0.0021	-8.27477 ± 0.00037
$2.4 - 2.6$	2.73576 ± 0.00007	2.9528 ± 0.0050	22.2672 ± 0.0025	-9.70000 ± 0.00045
$2.6 - 2.8$	3.07686 ± 0.00009	1.3971 ± 0.0060	26.1083 ± 0.0030	-11.21441 ± 0.00053
$2.8 - 3.0$	3.42154 ± 0.00010	-0.8065 ± 0.0073	30.2253 ± 0.0036	-12.82078 ± 0.00062
$3.0 - 3.2$	3.77003 ± 0.00011	-3.7322 ± 0.0087	34.5944 ± 0.0043	-14.52290 ± 0.00072
$3.2 - 3.4$	4.12234 ± 0.00013	-7.4886 ± 0.0104	39.2463 ± 0.0051	-16.32211 ± 0.00083
$3.4 - 3.6$	4.47856 ± 0.00015	-12.1418 ± 0.0124	44.1680 ± 0.0060	-18.21902 ± 0.00096
$3.6 - 3.8$	4.83866 ± 0.00017	-17.7410 ± 0.0148	49.3479 ± 0.0071	-20.21973 ± 0.00110
$3.8 - 4.0$	5.20174 ± 0.00019	-24.4027 ± 0.0177	54.8269 ± 0.0084	-22.31478 ± 0.00126
$4.0 - 4.2$	5.56775 ± 0.00021	-32.2591 ± 0.0212	60.5459 ± 0.0099	-24.51455 ± 0.00144
$4.2 - 4.4$	5.93670 ± 0.00024	-41.2980 ± 0.0254	66.5443 ± 0.0117	-26.81524 ± 0.00165
$4.4 - 4.6$	6.30921 ± 0.00027	-51.6850 ± 0.0304	72.8360 ± 0.0137	-29.22286 ± 0.00187
$4.6 - 4.8$	6.68288 ± 0.00030	-63.4745 ± 0.0365	79.3570 ± 0.0161	-31.72610 ± 0.00212
$4.8 - 5.0$	7.05892 ± 0.00033	-76.8683 ± 0.0440	86.2544 ± 0.0189	-34.33061 ± 0.00241
$5.0 - 5.2$	7.43726 ± 0.00037	-91.8648 ± 0.0530	93.3017 ± 0.0222	-37.04959 ± 0.00272
$5.2 - 5.4$	7.81707 ± 0.00041	-108.4015 ± 0.0639	100.7171 ± 0.0261	-39.86233 ± 0.00308
$5.4 - 5.6$	8.19870 ± 0.00046	-126.8290 ± 0.0774	108.3524 ± 0.0304	-42.78088 ± 0.00348
$5.6 - 5.8$	8.58279 ± 0.00051	-147.3051 ± 0.0940	116.3804 ± 0.0357	-45.81359 ± 0.00393
$5.8 - 6.0$	8.96735 ± 0.00057	-169.9489 ± 0.1139	124.6019 ± 0.0418	-48.94595 ± 0.00444
$6.0 - 6.2$	9.35345 ± 0.00063	-194.3185 ± 0.1394	133.1162 ± 0.0492	-52.18043 ± 0.00502
$6.2 - 6.4$	9.73840 ± 0.00069	-220.7647 ± 0.1712	141.9239 ± 0.0578	-55.51927 ± 0.00565
$6.4 - 6.6$	10.12738 ± 0.00077	-249.7792 ± 0.2091	151.0865 ± 0.0677	-58.96573 ± 0.00638
$6.6 - 6.8$	10.51659 ± 0.00085	-281.1153 ± 0.2561	160.3162 ± 0.0802	-62.52332 ± 0.00736
$6.8 - 7.0$	10.90541 ± 0.00094	-315.0544 ± 0.3112	170.1481 ± 0.0941	-66.16998 ± 0.00829
$7.0 - 7.2$	11.29740 ± 0.00104	-352.3613 ± 0.3820	180.2278 ± 0.1102	-69.93934 ± 0.00915
$7.2 - 7.4$	11.68581 ± 0.00115	-390.4128 ± 0.4679	189.9568 ± 0.1295	-73.79687 ± 0.01033
$7.4 - 7.6$	12.08266 ± 0.00128	-432.7892 ± 0.5839	200.9453 ± 0.1531	-77.80139 ± 0.01165
$7.6 - 7.8$	12.47254 ± 0.00141	-478.4916 ± 0.7052	211.5939 ± 0.1792	-81.87225 ± 0.01313
$7.8 - 8.0$	12.86991 ± 0.00156	-524.9324 ± 0.9245	223.0187 ± 0.2138	-86.09206 ± 0.01483
$8.0 - 8.2$	13.26321 ± 0.00172	-577.0701 ± 1.0982	234.3402 ± 0.2533	-90.38641 ± 0.01671
$8.2 - 8.4$	13.65319 ± 0.00190	-628.5931 ± 1.4289	245.7515 ± 0.3025	-94.76859 ± 0.01887
$8.4 - 8.6$	14.05098 ± 0.00211	-686.1360 ± 1.7585	257.7179 ± 0.3484	-99.29108 ± 0.02128
$8.6 - 8.8$	14.44353 ± 0.00232	-750.9577 ± 1.8829	270.1815 ± 0.4105	-103.89006 ± 0.02399
$8.8 - 9.0$	14.83704 ± 0.00257	-815.3002 ± 2.3285	283.1744 ± 0.4893	-108.57330 ± 0.02705
$9.0 - 9.2$	15.23688 ± 0.00283	-877.7905 ± 3.2236	296.2676 ± 0.6484	-113.44241 ± 0.03055
$9.2 - 9.4$	15.63060 ± 0.00313	-954.9899 ± 3.8191	308.4226 ± 0.7593	-118.36857 ± 0.03441
$9.4 - 9.6$	16.03193 ± 0.00346	-1030.7033 ± 4.4742	322.0296 ± 0.8728	-123.46222 ± 0.03884
$9.6 - 9.8$	16.42336 ± 0.00383	-1108.4613 ± 4.8676	336.9731 ± 0.9487	-128.52130 ± 0.04392
$9.8 - 10.0$	16.82386 ± 0.00423	-1188.7666 ± 8.4394	350.7993 ± 1.3343	-133.89305 ± 0.04955
$10.0 - 10.2$	17.22008 ± 0.00467			-139.24776 ± 0.05602
$10.2 - 10.4$	17.61896 ± 0.00517			-144.67924 ± 0.06332
$10.4 - 10.6$	18.01720 ± 0.00571			-150.24974 ± 0.07139
$10.6 - 10.8$	18.41918 ± 0.00631			-156.05150 ± 0.08068
$10.8 - 11.0$	18.81383 ± 0.00695			-161.75693 ± 0.09050
$11.0 - 11.2$	19.22148 ± 0.00771			-167.73174 ± 0.10267
$11.2 - 11.4$	19.60535 ± 0.00848			-173.55084 ± 0.11589
$11.4 - 11.6$	20.00483 ± 0.00939			-179.76825 ± 0.13097
$11.6 - 11.8$	20.40568 ± 0.01040			-185.96573 ± 0.14723
$11.8 - 12.0$	20.82530 ± 0.01146			-192.55302 ± 0.16694

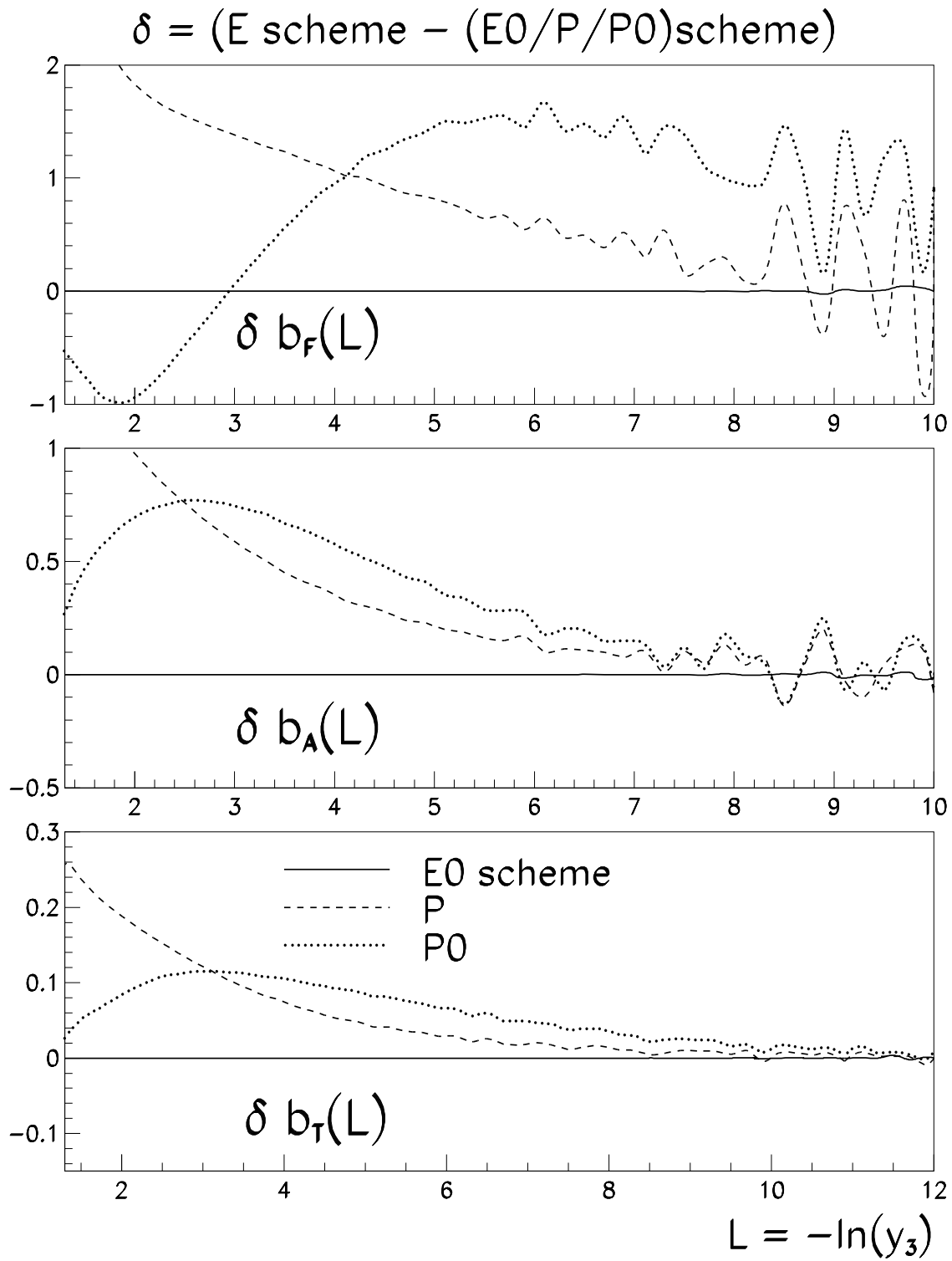Table 2: Monte Carlo results for coefficients a, b_F, b_A and b_T.

Figure 1: Absolute differences between the coefficients $b_*(L)$ obtained from a Monte Carlo integration for the various recombination schemes.
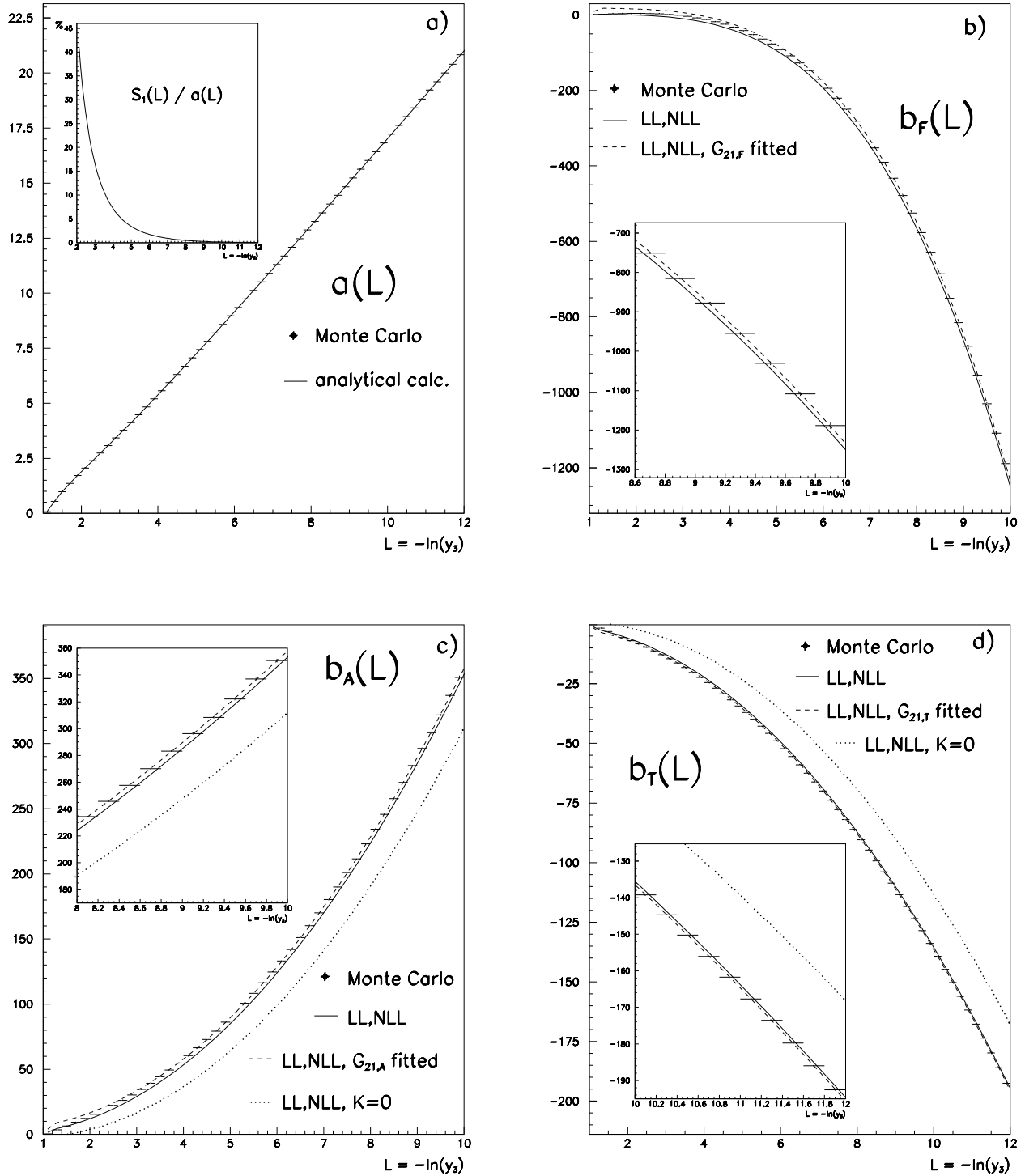
Figure 2: a) First order coefficient $a(L)$ obtained by Monte Carlo compared to the analytical result. The inset shows the relative contribution of the non-logarithmic terms to the full first order prediction. b–d) Second order coefficients $b_*(L)$. Plotted are the Monte Carlo result, the predictions obtained from all known LL and NLL terms, the (LL,NLL) predictions improved by the addition of the fitted subleading coefficients $G_{21,*}$ and the incomplete (LL,NLL) predictions ($K = 0$).
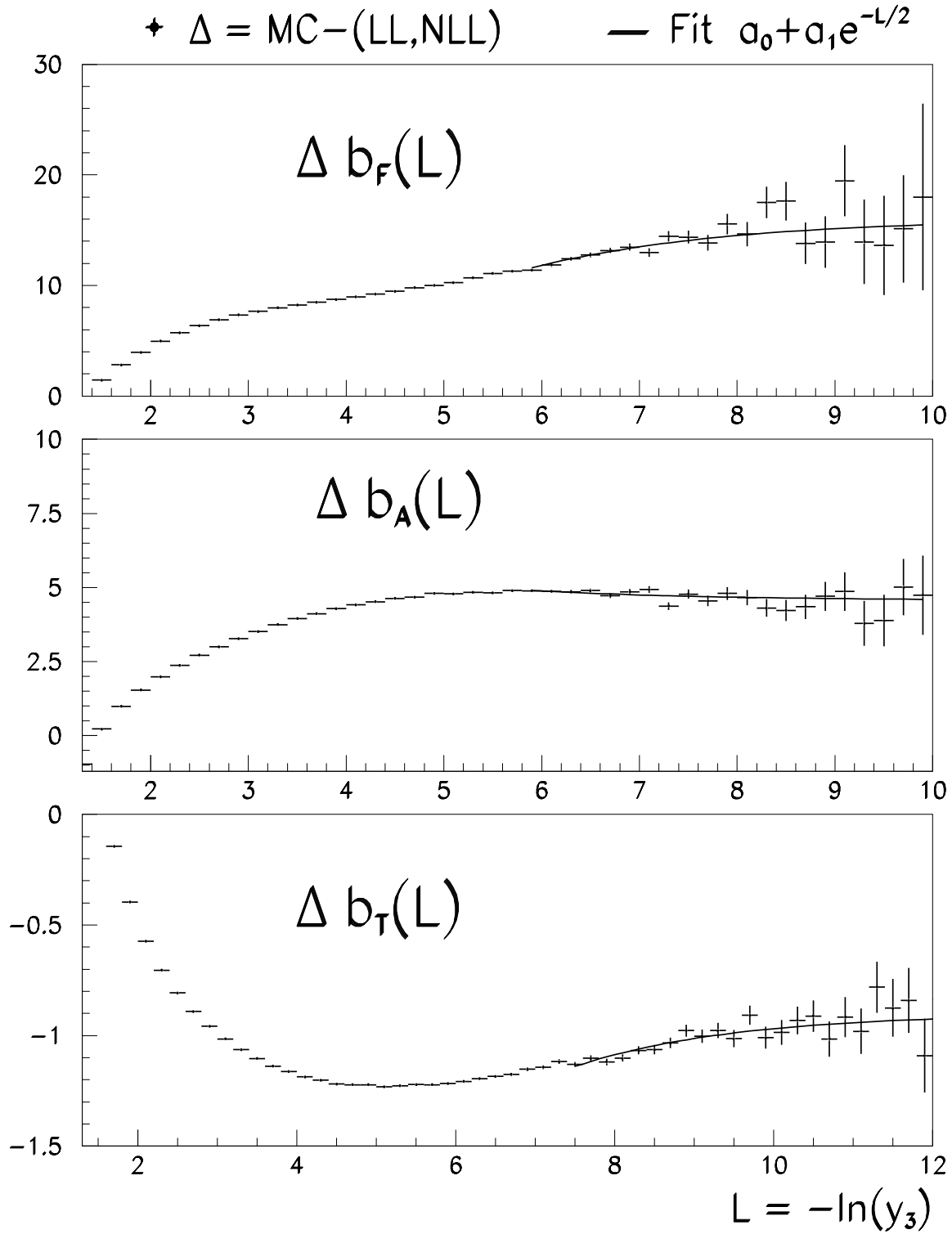
11

Figure 3: Differences between the Monte Carlo integration and all known LL and NLL terms for the second order coefficients $b_*(L)$. The lines show the fitted functions $a_0 + a_1 e^{-L/2}$ over the range used in the fit.

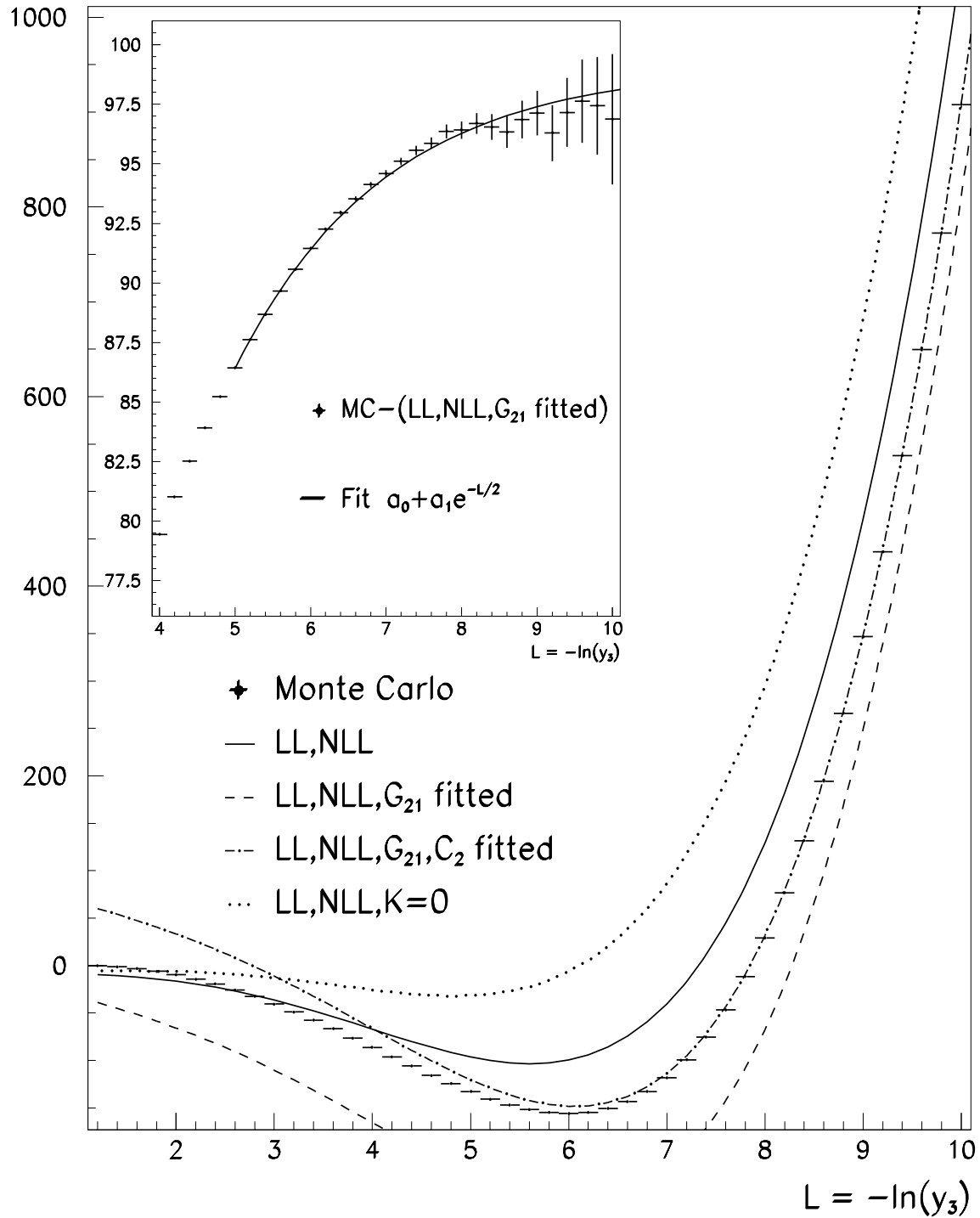# Second order QCD coefficient of $R_2(L)$

Figure 4: The second order coefficient of the cumulative 2–jet rate. Plotted are the Monte Carlo result and variations of the (LL,NLL) calculation, taking into account also the known subleading coefficient C_1. The inset shows the difference between the Monte Carlo integration and all known LL,NLL and subleading terms, as well as a fit of its asymptotic tail.